The EMBO Journal Vol. 20 No. 13 pp. 3370–3379, 2001

Analysis of heterodimer formation by Xklp3A/B, a newly cloned kinesin-II from *Xenopus laevis*

Valeria De Marco, Peter Burkhard[1], Nathalie Le Bot[2], Isabelle Vernos[2] and Andreas Hoenger[3]

EMBL Structural and Computational Biology Programme and [2]EMBL Cell Biology and Cell Biophysics Programme, Meyerhofstrasse 1, 69117 Heidelberg, Germany and [1]Biozentrum der Universität Basel, Abteilung Strukturbiologie, Klingelbergstrasse 70, 4056 Basel, Switzerland

[3]Corresponding author
e-mail: hoenger@embl-heidelberg.de

kinesin-II motor proteins are composed of two different kinesin-like motor proteins and one cargo binding subunit. Here we report the cloning of a new member of the kinesin-II superfamily, Xklp3A from *Xenopus laevis*, which forms a heterodimeric complex with Xklp3B. The heterodimer formation properties between Xklp3A and B have been tested *in vitro* using reticulocyte lysate expression and immunoprecipitation. To this end we produced a series of Xklp3A and B constructs of varying length and tested their propensity for heterodimer formation. We could demonstrate that, in contrast to conventional kinesin, the critical domains for heterodimer formation in Xklp3A/B are located at the C-terminal end of the stalk. Neither the neck nor the highly charged stretches after the neck region, which are typical of kinesins-II, are required for heterodimer formation, nor do they prevent homodimer formation. Dimerization is controlled by a cooperative mechanism between the C-terminal coiled-coil segments. Classical trigger sites were not identified. The critical regions for dimerization exhibit a very high degree of sequence conservation among equivalent members of the kinesin-II family.

Keywords: α-helical coiled coil/coiled-coil trigger site/heptad repeats/kinesin-II/Xklp3A/B

Introduction

Since the discovery of the first member of the kinesin superfamily by Brady (1985) and Vale *et al*. (1985) our knowledge about kinesin and kinesin-like relatives has expanded tremendously (for a review see Hirokawa, 1998). Despite their diverse functions at various locations throughout the cell, the motor domains of kinesin molecules exhibit extended homologies within their primary sequences and even more striking similarities within their three-dimensional configuration of secondary structure elements (Sack *et al*., 1999). The most variable parts in kinesins are found within the domains involved in cargo interaction, which specialize them for their particular cellular tasks. An additional level of specification can be found in variations of oligomerization motives between (several) kinesin motors and cargo domains. Although homodimeric motors such as conventional kinesin or ncd are most common, monomeric, tetrameric and heterotrimeric motors have now been identified as well (Hirokawa, 1998).

Cole *et al*. (1993) isolated the first heterotrimeric motor molecule from sea urchin embryo extracts. kinesin-II forms a heterotrimeric complex composed of two related (but not identical) kinesin-like motors (spKRP85 and spKRP95; Rashid *et al*., 1995) and a non-motor accessory subunit (spKAP115; Wedaman *et al*., 1996). Meanwhile, several homologues of the sea urchin kinesin-II complex have been identified in species ranging from *Chlamydomonas* to humans (Marszalek and Goldstein, 2000). Additional motor proteins, distinct from the classical kinesin-II motor components, have been discovered recently in mammals (Muresan *et al*., 1998; Yang and Goldstein, 1998) and in *Caenorhabditis elegans* (Tabish *et al*., 1995; Signor *et al*., 1999a). Functional kinesin-II complexes show an interesting modular variability in their composition between various motor and cargo binding subunits, thus yielding isoforms that are highly specialized and adaptable to different tissues and/or subcellular localization (Muresan *et al*., 1998; Yang and Goldstein, 1998). kinesin-II has been found to move along microtubules in an anterograde direction completing several different tasks. In close collaboration with cytoplasmic dynein, kinesin-II is involved in the construction and maintenance of cilia and flagella (Brown *et al*., 1999; Signor *et al*., 1999b). Defects in kinesin-II have been described as causing non-functional cilia, which, among other effects, disturb the left–right asymmetry in mice during embryogenesis due to an inhibited nodal flow (Morris and Scholey, 1997; Cole *et al*., 1998; Nonaka *et al*., 1998; Rosenbaum *et al*., 1999). Other functions include neuronal transport (Kondo *et al*., 1994; Ray *et al*., 1999), melanosome transport (Tuma *et al*., 1998) and organelle trafficking (Le Bot *et al*., 1998) (for a review see Marszalek and Goldstein, 2000).

Based on sequence analysis, the domain organization of the two chains containing the motor portion of kinesin-II resembles that of conventional kinesin heavy chain. Both are N-terminal motors, which are typical of anterograde kinesins. The globular domains contain the microtubule and nucleotide binding sites and connect via a rod-shaped stalk to a C-terminal tail, which binds to an accessory unit or so-called kinesin-associated protein (KAP; Scholey, 1996). In most parts the stalk is formed by a heterodimeric coiled coil (~240 amino acids; Figure 2). A unique feature at the beginning of the kinesin-II stalks are highly charged regions that exhibit opposite polarity from one chain to the other and interrupt the coiled coil between the neck and the remaining stalk. These oppositely charged regions have

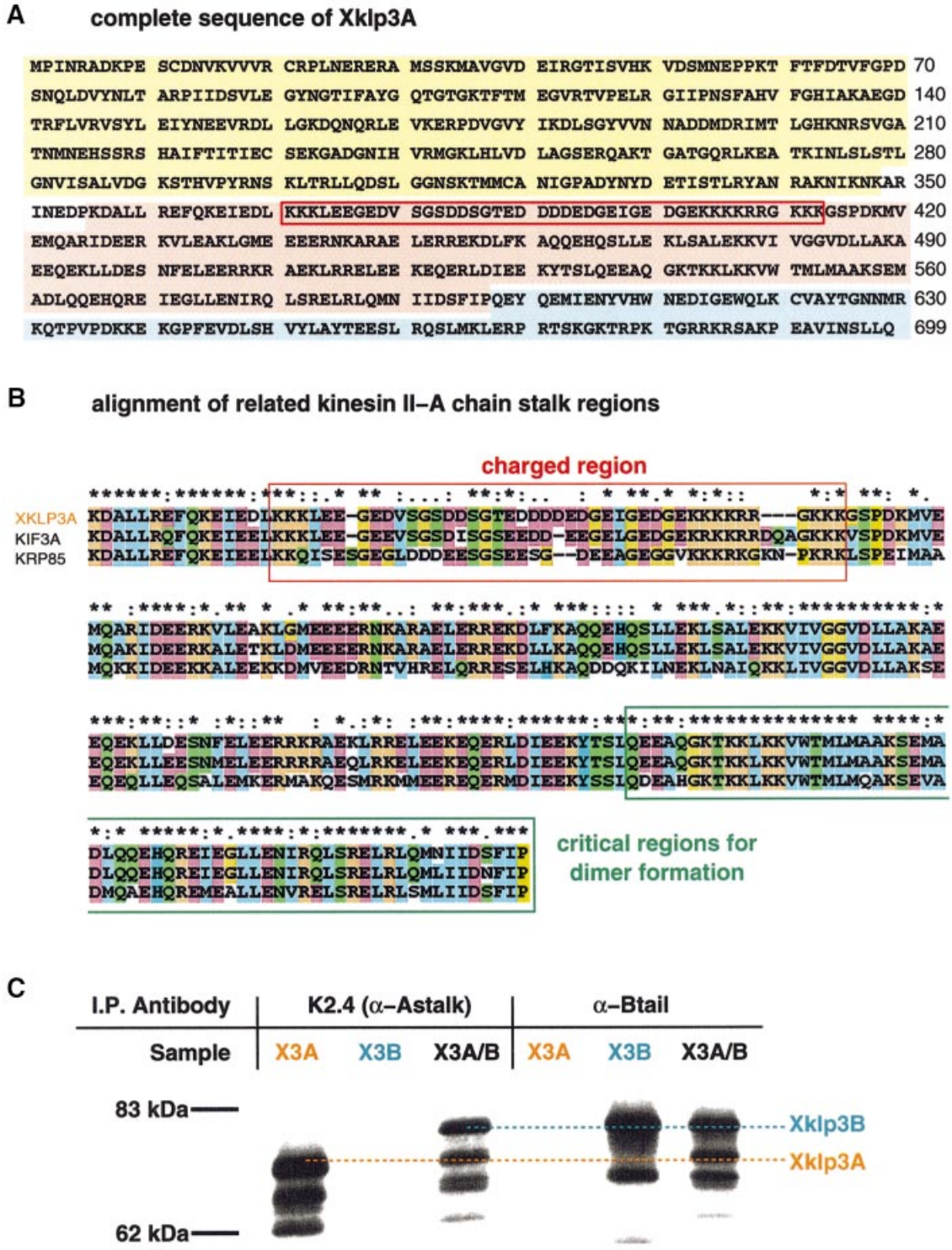

Fig. 1. Xklp3A belongs to the kinesin II family and forms a complex with Xklp3B. The predicted protein sequence of Xklp3A is shown in (**A**). Domains are marked as follows: motor domain, yellow; stalk region, pink; tail domain, blue. A red frame marks the stretch of highly charged amino acids that separates the neck from the coiled-coil stalk. (**B**) The predicted sequence for the stalk region in Xklp3A is aligned with MmKIF3A and SpKRP85: identical residues are marked with an asterisk (*), conserved residues with double dots (:), semi-conserved residues with a single dot (.). The colour code distinguishes between non-polar amino acids (blue), polar (green) and charged residues (orange for positively charged, purple for negatively charged). The alignment was performed using ClustalX. Interestingly the critical region for dimerization (C-terminal part of the stalk) is highly conserved among related members of the kinesin II family. (**C**) Immunoprecipitation of Xklp3A/B heterodimer: an α-Astalk antibody (K2.4: raised against the stalk of SpKRP85) precipitates Xklp3A but not Xklp3B unless they are co-expressed and a complex between the two kinesin-like proteins is formed. Consequently an α-Xklp3B antibody (α-Btail) immunoprecipitates Xklp3A only when expressed with Xklp3B.

been proposed to play a key role in the formation of a heterodimeric complex (Rashid *et al*., 1995). Here we present the cloning of a novel member of the kinesin-II subfamily, Xklp3A, and our investigations into the heterodimer formation between Xklp3A and Xklp3B (Vernos *et al*., 1993; Le Bot *et al*., 1998; Tuma *et al*.,

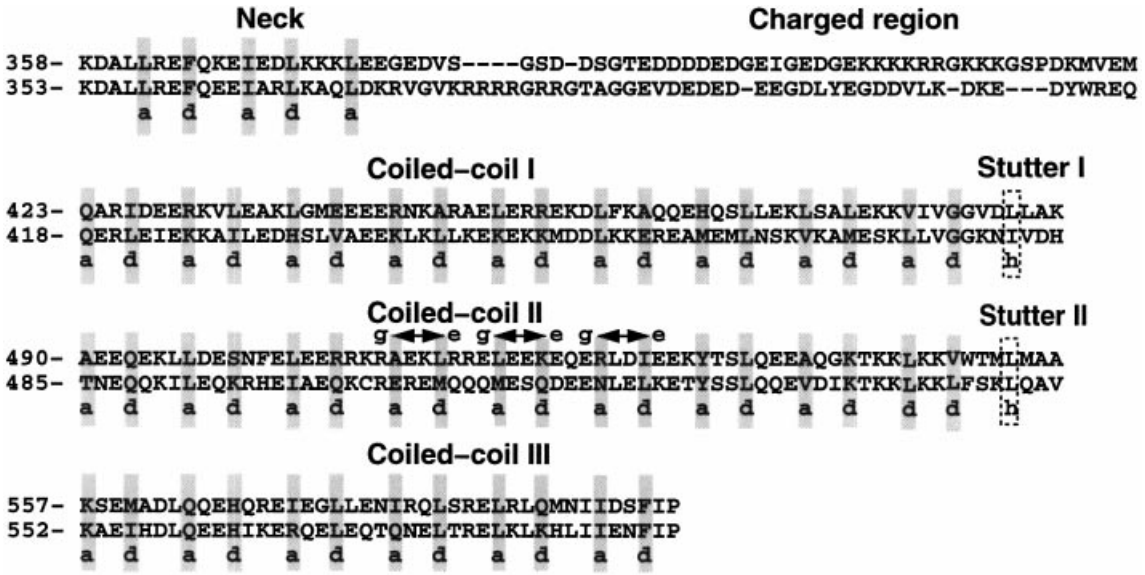

Fig. 2. Xklp3A and Xklp3B show a tripartite organization of the stalk domain. Heptad-repeat assignment for Xklp3A and Xklp3B stalks, as predicted by Multicoil and visual inspections, reveals three coiled-coil subdomains, connected through stutters (Brown *et al*., 1996). The neck region is separated from the coiled-coil stalk by the charged region. The neck and in particular the charged regions are not predicted to fold in a stable coiled coil. Arrows mark repulsive e–g ionic interactions in Xklp3A coiled-coil region II, which could prevent homodimerization.

1998). Our own work identifies distinct areas of the Xklp3A and B stalks as being essential for maintaining a stable coiled coil. In contrast to conventional kinesin, these areas locate at the C-terminal end of the stalk. Dimer formation is not controlled by a trigger sequence (Kammerer *et al*., 1998; Thormählen *et al*., 1998) or trigger site (Steinmetz *et al*., 1998; Burkhard *et al*., 2000a). Instead, Xklp3A/B dimer formation appears to be regulated by a cooperative mechanism involving the final two coiled-coil segments of the stalk. Moreover, our data rule out a significant role for the charged stretches and the neck in the process of heterodimer formation.

Results

Xklp3A is a novel member of the kinesin-II subfamily and forms a complex with Xklp3B

Xklp3A was isolated using a combination of cDNA library screening and a PCR-based cloning strategy (see Materials and methods). The clone was found to have one open reading frame of 2097 bp encoding a polypeptide chain of 699 amino acids with the predicted molecular weight of 79 700 Da (Figure 1A). Sequence analysis revealed the typical domain organization of kinesin-like proteins, with an N-terminal motor domain, containing the nucleotide and the microtubule binding sites, linked to the C-terminal tail by a coiled-coil stalk (Figures 1A and 7). A BLAST search with Xklp3A-predicted protein sequence confirmed a high homology with other members of the kinesin-II subfamily: Xklp3A exhibits 68% identity to SpKRP85 and 92% to the mouse KIF3A. An alignment of Xklp3A neck and stalk with the homologous regions in SpKRP85 and MmKIF3a is shown in Figure 1B. Like its relatives, Xklp3A exhibits a predicted coiled-coil stalk, which is interrupted by a stretch of highly charged residues (Figure 1B). The charge distribution of this sequence is complementary to the charged stretch of Xklp3B (see Figure 7). Heterodimerization between Xklp3A and B has been tested by immunoprecipitation, using antibodies against the stalk regions of Xklp3A and B (Figure 1C). Xklp3A and Xklp3B were either translated independently or co-expressed in a rabbit reticulocyte lysate system (Figure 1C). Xklp3B was immunoprecipitated by an antibody raised against the Xklp3A homologue SpKRP 85 (Cole *et al*., 1993), only in the presence of Xklp3A, and vice versa, Xklp3A was immunoprecipitated by an α-Xklp3B antibody (Le Bot *et al*., 1998) only when expressed together with Xklp3B (Figure 1C). This clearly confirmed that Xklp3A is a partner of Xklp3B in the *Xenopus* kinesin-II complex and that they form a stable complex *in vitro*.

The Xklp3A/B coiled-coil assignment unveils three discrete regions within the stalk

Coiled-coil predictions on the Xklp3A and Xklp3B stalks were carried out using the program Multicoil (Wolf *et al*., 1997) developed for the prediction of homodimeric and trimeric coiled coils. To overcome the limitations of the prediction programs available for heterodimeric coiled coils, we further improved the heptad-repeat assignment by visual inspection of the sequence. According to the program Multicoil, the region that corresponds to the neck in conventional kinesin has only a low tendency (20%) to form a coiled coil, while the charged regions, which contain many glycine residues, do not fold into a coiled coil (Figure 2). The resulting heptad-repeat assignment reveals three consecutive coiled-coil regions located at the C-terminal end of the charged region. Despite slight ambiguity about the secondary structure predictions of these regions, the most plausible assignment of the three coiled-coil segments of the stalk domain is as follows: the first region spans residues 423–480 in Xklp3A and residues 418–475 in Xklp3B, respectively. The heptad-repeat assignment for this segment seems to be the least

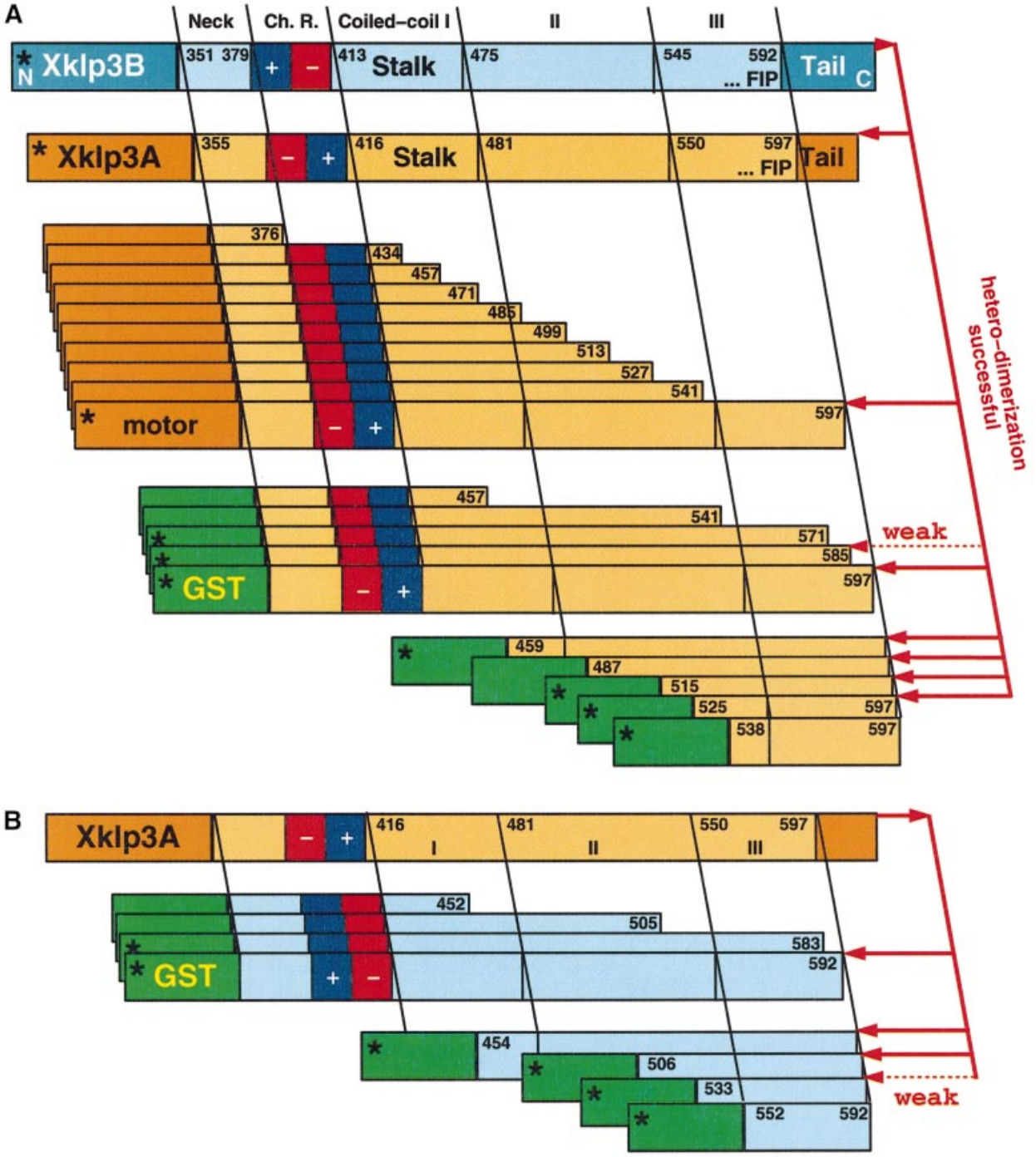

Fig. 3. Schematic overview of the constructs, which were probed for heterodimer formation. (**A**) Heterodimer formation of full-length Xklp3B chain was tested against Xklp3A constructs with various stalk fragments. Xklp3A/B heterodimer formation occurs only when the C-terminal part of Xklp3A stalk is present. N-terminal truncations allow complete omission of the neck, the charged regions (Ch. R.), coiled-coil region I and most of coiled-coil region II. In some experiments the motor head was exchanged with a GST domain, which allowed for a more effective immunoprecipitation. This did not change the outcome of the precipitation experiments and revealed identical results (see Figures 4–6). (**B**) The reversed experimental set-up of (A). Confirming the findings made with Xklp3A segments, the C-terminal part of Xklp3B stalk is equally essential for heterodimer formation. The asterisks mark constructs of which immunoprecipitation results are shown in Figures 4–6.

ambiguous and mainly identical for both chains of the heterodimer (Figure 2). The second coiled-coil region extends from residue 490 to 550 in Xklp3A, corresponding to residues 485–545 in Xklp3B. The third coiled-coil segment can be assigned to the residues ranging from 557 to 597 in Xklp3A and from 552 to 592 in Xklp3B. In the assignment presented the three segments appear to be linked by two so-called coiled-coil stutter sequences (marked with frames in Figure 2; Brown *et al*., 1996).

Xklp3A/B heterodimer formation is initiated by the C-terminal part of the stalk

As the *in vitro* coupled transcription and translation system worked efficiently to demonstrate Xklp3A/B complex

formation, we decided to use the method for a rapid identification of the regions involved in heterodimer formation. Moreover, the studies of Rashid *et al*. (1995) and Yamazaki *et al*. (1995) were highly valuable for this particular work as they both used the same *in vitro* systems applied here to establish that the two motor subunits of KRP85/95 and KIF3A/B co-assemble directly via their coiled-coil domains, and that the KAP is not required for heterodimer formation.

The coiled-coil neck region of conventional kinesin has been shown to be sufficient to initiate homodimer formation between two heavy chains (Kozielski *et al*., 1997; Morii *et al*., 1997). The equivalent region in kinesin-II, however, is less likely to form a stable coiled coil. The neck is followed by a highly charged region, which exhibits no coiled-coil propensity at all. The arrangement of charges in A and B shows an opposite polarity, which led to speculations about a functional involvement in heterodimer partner recognition and homodimer prevention (Rashid *et al*., 1995). Here, we decided to test whether this region indeed plays a crucial role in heterodimer formation or whether additional parts are essential for complex formation. Based on the dimerization properties found in conventional kinesin we gradually elongated the stalk of Xklp3A up to its full length to find the shortest possible construct that forms heterodimers (Figure 3A). Each truncated Xklp3A construct was co-translated with Xklp3B in the reticulocyte system and the complex formation was tested by immunoprecipitation either with the α-KRP85 antibody or with the α-Xklp3B antibody. The constructs used for immunoprecipitations are illustrated in Figure 3. Starting off with the shortest construct (Xklp3A:N-376; N stands for the N-terminal end of the stalk, including the neck, starting at residue 355), which lacked the charged region and the entire C-terminal stalk, we gradually elongated the stalk as shown in Figure 3. To our surprise none of the constructs was able to form a complex with Xklp3B until the complete stalk was restored (Xklp3A:N-597: compare with Xklp3A:N-541 in Figures 3A and 4A). This was clearly identifying C-terminal regions of the stalk rather than the N-terminal neck as crucial for dimerization. Neither the neck alone, the neck plus the charged region nor even those constructs that contain a substantial N-terminal fraction of the coiled-coil region, were able to form heterodimers with Xklp3B (Figures 3 and 4A).

In a next step we checked whether the removal of the motor domain would affect heterodimerization by substituting the motor part with a glutathione *S*-transferase (GST) domain (GST-A:N-597; see Figures 3A and 4B). We could show that the GST-A:N-597 construct behaved equivalently to the Xklp3A:N-597 in promoting heterodimerization, thus showing that the motor heads are not involved in heterodimer stabilization (Figure 4B). We then created GST fusion constructs of the Xklp3A:N-457 and Xklp3A:N-541 constructs (Figure 3A), which replaced the motor head with a GST domain and tested heterodimer formation by using an α-GST antibody (Wittmann *et al*., 1998). This series of experiments clearly confirmed that truncating C-terminal parts of the stalk abolished heterodimer formation. In order to better define the region necessary for complex formation we deleted first four and then two heptad repeats from the C-terminal coiled-coil

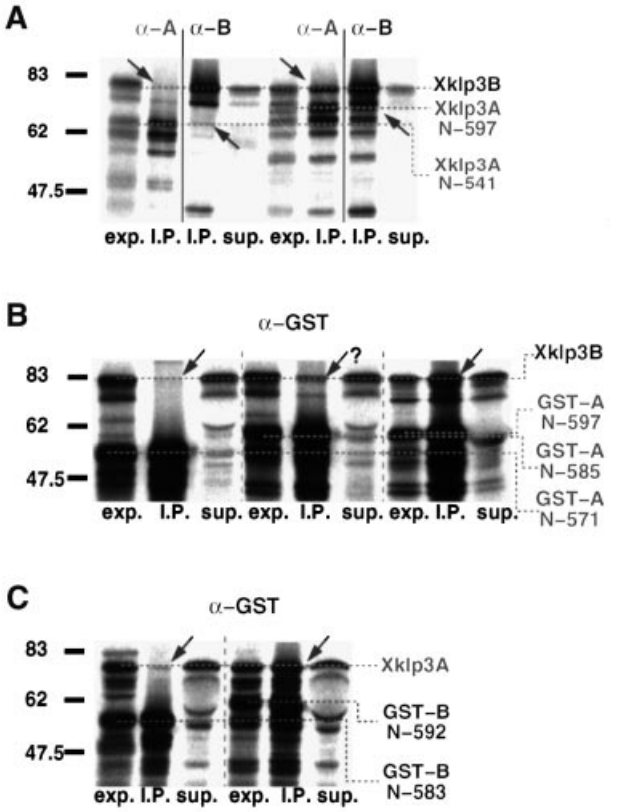

Fig. 4. Heterodimer formation is 'triggered' by the C-terminal part of the stalk. (**A**) The removal of even a short part of the C-terminal end of the Xklp3A stalk inhibits heterodimer formation. Xklp3B was co-expressed with Xklp3A:N-541 (left lanes) or Xklp3A:N-597 (right lanes). Complex formation was monitored by immunoprecipitation using both α-SpKRP85 (α-A) and α-Xklp3B (α-B) antibodies. The construct with full-length stalk is the only one precipitated through heterodimer formation. (**B**) Even short truncations of the Xklp3A coiled-coil region III from the C-terminal end inhibit coiled-coil formation. Xklp3B was co-expressed with GST-A:N-571, GST-A:N-585 and GST-A:N-597. Only GST-A:N-597 is fully capable of precipitating Xklp3B. Complex formation was tested by immunoprecipitation with an α-GST antibody. (**C**) In analogy to the experiments shown in (B), truncation of the Xklp3B coiled-coil region III destabilizes dimer formation in a very similar way. Xklp3A was co-expressed with GST-B:N-583 or GST-B:N-592 and precipitated with α-GST. GST-B:N-583 is already too short to form a heterodimeric complex. Lanes are marked as follows: exp., lysate before immunoprecipitation; I.P., immunoprecipitate; sup., supernatant after precipitation. Arrows mark the position of products coprecipitated via heterodimer formation. Compare also with Figure 3.

breaker Phe-Ile-Pro (FIP) motif (see Figure 2), which marks the end of the predicted α-helical coiled coil. We found that a C-terminal truncation of the stalk by only two heptad repeats decreased the possibility of dimer formation substantially (GST-A:N-585; Figure 4B), and removing four repeats completely abolished dimerization (GST-A:N-571; Figure 4B).

We then tested whether similar results could be obtained by removing the C-terminal part of the stalk in Xklp3B. To this end we designed GST-B:N-452, GST-B:N-505, GST-B:N-583 and GST-B:N-592 fusion proteins (Figure 3B) and tested the possibility of heterodimer formation by immunoprecipitation with an α-GST antibody: GST-B:N-452, GST-B:N-505 and GST-B:N-583 all failed to form heterodimers whereas the complex was

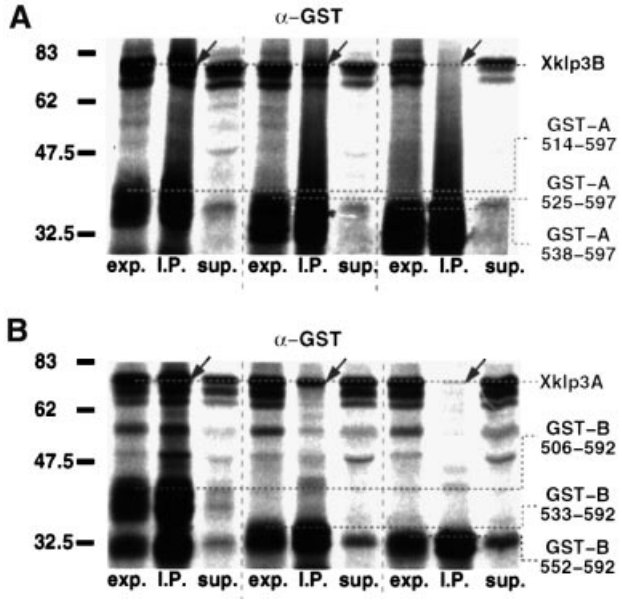

Fig. 5. Heterodimer formation is controlled by a cooperative interaction between coiled-coil regions II and III. (**A**) Xklp3B was co-expressed with GST-A:514–597 (leaves five complete C-terminal heptads of coiled-coil region II), GST-A:525–597 (four heptads left) or with GST-A:538–597 (two heptads left). GST-A:525–597 shows a lower efficiency in complex formation, and GST-A:538–597 is incapable of forming a heterodimer. As in Figure 4B and C heterodimer formation was monitored by immunoprecipitation with an α-GST antibody. (**B**) Reversing the conditions from (A), Xklp3A was co-expressed with GST-B:506–592 (six heptads left), GST-B:533–592 (two heptads left) or GST-B:552–592 (complete coiled-coil region III). In this case slightly shorter stretches are still showing some heterodimer formation. GST-B:506–592 is fully capable, GST-B:533–592 is much less capable and GST-B:552–592 is incapable of heterodimer formation. Lanes are marked as follows: exp., lysate before immunoprecipitation; I.P., immunoprecipitate; sup., supernatant after precipitation. Arrows mark the position of products coprecipitated via heterodimer formation.

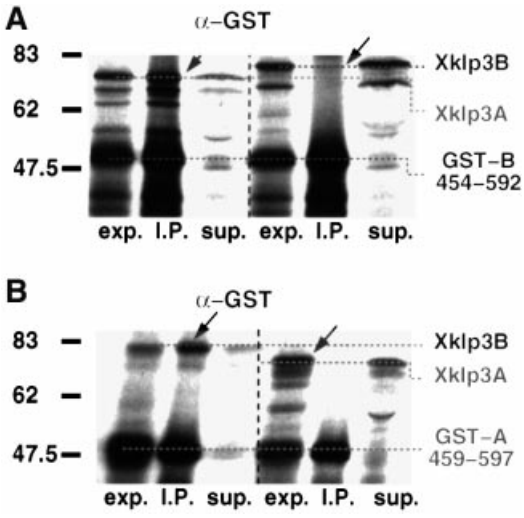

Fig. 6. The removal of Xklp3A and Xklp3B charged regions does not affect heterodimer formation and does not promote homodimerization of the two subunits. (**A**) GST-B:454–592, lacking the N-terminal regions between the beginning of the neck and the end of the charged regions, was co-expressed either with Xklp3A or Xklp3B. As in Figures 3 and 4 complex formation was checked by immunoprecipitation with α-GST. Complex formation occurs only between GST-B:454–592 and Xklp3A (left lanes) but not between GST-B:454–592 and Xklp3B (right). (**B**) Vice versa, GST-A:459–597 was co-expressed with either Xklp3A or Xklp3B. As in (A) α-GST precipitates only a complex that is formed between GST-A:459–597 and Xklp3B (left) but not between GST-A:459–597 and Xklp3A (right). Lanes are marked as follows: exp., lysate before immunoprecipitation; I.P., immunoprecipitate; sup., supernatant after precipitation. Arrows mark the position of products coprecipitated via heterodimer formation.

formed when the full stalk was present (GST-B:N-592) (compare GST-B:N-583 with GST-B:N-592 in Figure 4C).

Heterodimer formation requires part of coiled-coil region II and the complete region III

Finally, we attempted to identify the shortest possible coiled-coil region that is still able to form heterodimers. To this end we designed constructs in which heptad repeats were progressively removed from the N-terminal side of the stalk (Figure 3). As described above, complex formation was tested by immunoprecipitation with an α-GST antibody. We could demonstrate that heterodimer formation was still unaffected after truncation of the entire coiled-coil region I (Figures 2 and 3A). Moreover, we could show that even the N-terminal part of coiled-coil II is not essential for complex formation. Finally, heterodimer formation is inhibited when coiled-coil segment II is truncated to a residual length of less than four heptads (compare GST-A:514–597 with GST-A:538–597 in Figure 5A).

As expected, truncation of the Xklp3B stalk from the N-terminal side revealed very similar results (Figure 5B). Our data clearly demonstrate that coiled-coil formation is initiated by two adjacent coiled-coil regions at the C-terminus of Xklp3A and Xklp3B stalks (see Figure 7), and that the removal or truncation of either of the two interferes with complex formation. The critical regions for heterodimer formation exhibit a remarkable conservation among analogous members of the kinesin-II family. The neck and charged stretches, on the other hand, show a much lower degree of homology (see Figure 1B).

The charged regions are not required for heterodimer formation

Based on the results above, the charged regions did not appear to be involved in stabilizing the heterodimeric coiled-coil stalk. However, we decided to investigate further the effect of their removal from the stalk on the formation of homodimers. To check for homodimerization, Xklp3A was co-expressed with GST-A:459–597 and Xklp3B was co-expressed with GST-B:454–592 (Figure 6). The interaction was monitored by immunoprecipitation using the α-GST antibody. Our results were unambiguous. Neither Xklp3A nor Xklp3B proved to be able to form homodimers, while in the control reactions (Xklp3A/GST-B:454–592; Xklp3B/GST-A:459–597) the complex formation could be established (Figure 6A and B). This pretty much excludes the charged regions from any significant role in heterodimer formation.

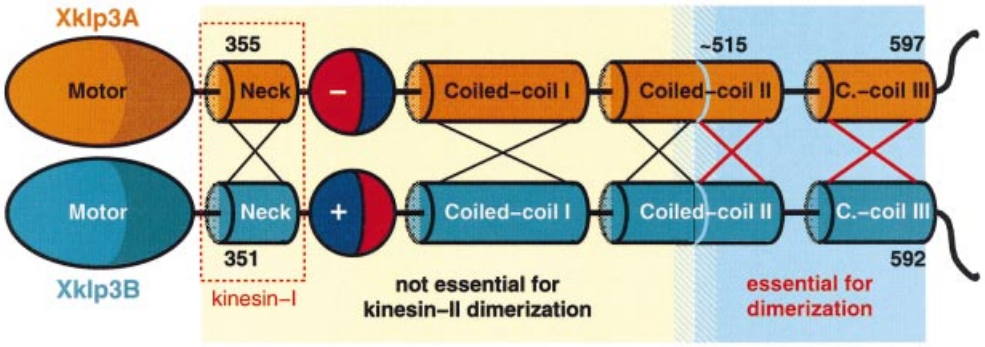

Fig. 7. Xklp3A/B heterodimer formation appears to be based on a cooperative mechanism between the C-terminal part of coiled-coil region II and the entire coiled-coil region III. Coiled-coil region II needs to maintain a minimum length of about two to three heptad repeats otherwise heterodimer formation is inhibited. Four remaining heptads restore full activity. Here we illustrate the key difference between dimerization of kinesin-II and of conventional kinesin. In contrast to the situation in conventional kinesin, the neck regions (red box) are not responsible for dimerization. Xklp3A/B heterodimerization is driven by the C-terminal part of the stalk. The sequences at the N- or C-terminal end of the blue region do not exhibit any coiled-coil trigger sequences. The absence of trigger sites and the involvement of two separated coiled-coil regions strongly suggest that dimerization is mediated by a cooperative mechanism that raises the relatively low individual coiled-coil-forming propensities of regions II and III to a physiologically significant level.

Discussion

Cloning of Xklp3A

In order to investigate the structure and function of the Xklp3A/B heterodimer we cloned the full-length polypeptide chain of Xklp3A (Figure 1A). Together with the B chain obtained earlier (Le Bot *et al*., 1998) we now have the full heterodimeric motor domain of Xklp3A/B available for further investigations of the structure and function of Xklp3A/B. The full sequence of Xklp3A shows strong homologies to its related members of the kinesin-II family KIF3A (Yamazaki *et al*., 1995) and KRP85 (Cole *et al*., 1993) (see Figure 1B). We made several attempts to purify the heads of Xklp3A and B separately using either *Escherichia coli* or insect cell expression systems, which have been successfully applied to obtain the head domains of conventional kinesin or ncd. However, irrespective of an accurate investigation of the motor domain and neck boundaries we could not obtain soluble products of any of the two heads or the stalks so far, which would be needed, e.g. for CD spectroscopy. The reasons for this behaviour are unclear as yet, but may be related to the unique dimerization properties of kinesin-II found here. We are currently establishing co-expression experiments to investigate further the mechanism of Xklp3A/B heterodimer formation.

Coiled-coil assignment

It is widely accepted within the scientific community that kinesins dimerize via coiled-coil formation. Electron microscopy data (e.g. see Hirokawa, 1998; heads and cargo domain are connected by a thin 3–4 μm long stalk, similar to conventional kinesin) and sequence analysis of the stalk region strongly suggest that this is also the case for kinesin-II heterodimers. The assignment of heptad repeats in the stalk regions of Xklp3A/B is a combination of predictions according to the program Multicoil (Wolf *et al*., 1997) and an assignment based on visual inspection to correct for heterodimeric coiled-coil formation. The Xklp3A/B stalk can be divided into an N-terminal neck region, analogous to conventional kinesin, a non-helical charged stretch and three additional coiled-coil regions towards the C-terminus, which are connected by two so-called coiled-coil stutters (Brown *et al*., 1996; Figure 2). The C-terminal ends of the third coiled-coil region are almost identical in both chains and terminate the coiled coil with a FIP motif. The proline residue marks the end of the coiled-coil formation and the transition into the KAP binding tail (Scholey, 1996). However, a more detailed investigation will require a high-resolution structure of the coiled-coil domain, as is available, for example, for the coiled-coil domain of cortexillin I (Burkhard *et al*., 2000a).

We have shown that heterodimer formation of Xklp3A and B requires two distinct coiled-coil regions at the ends of the coiled-coil regions II and III, respectively. It is striking that in Xklp3A the first region responsible for heterodimerization contains three consecutive repulsive g–e′ ionic interactions (see Figure 2). Hence, Xklp3A is expected to disfavour homodimer formation. Upon heterodimer formation with Xklp3B, however, these repulsive ionic interactions are largely relieved and in one case even replaced by an attractive ionic interaction (A Glu324–B Lys324′). On the other hand, the coiled-coil-forming propensity of Xklp3B in this region is rather low. Therefore, also Xklp3B by itself is not expected to form homodimers. This is confirmed by our most recent results when we attempted to purify the critical stalk regions of Xklp3A and B for crystallization. Only the A chain is reasonably stable on its own, suggesting that B forms around a template structure provided by A. Very recently, Arndt and coworkers have presented a very similar ‘strategy’ for preferential heterodimer formation by destabilizing the respective homodimers (Arndt *et al*., 2000).

The second critical region for heterodimeric coiled-coil formation at the C-terminal end of the coiled-coil segment III contains a stretch of six hydrophobic residues in a and d positions that strongly stabilize coiled coils (Tripet *et al*., 2000). This sequence, however, is lacking any stabilizing ionic interactions (Burkhard *et al*., 2000b). Consequently, removing only a few residues at the

C-terminal end of this stretch reduces the coiled-coil-forming propensity below a critical level and abolishes detectable coiled-coil formation. A similar effect has been observed at near-atomic resolution for coiled-coil segment 1A in intermediate filaments (Strelkov *et al*., 2001). This segment lacks any attractive ionic interaction, and despite a number of coiled-coil stabilizing hydrophobic residues at a and d positions fails to form a coiled coil but rather stays a monomeric α-helix (Strelkov *et al*., 2001).

Xklp3A/B heterodimerization is accomplished by a cooperative mechanism involving coil III and the C-terminal part of coil II

The rationale for our initial experiments was based on the dimerization properties of conventional kinesin (Morii *et al*., 1997; Marx *et al*., 1998; Thormählen *et al*., 1998) and on the prediction made for the charged regions in kinesin-II (Rashid *et al*., 1995). In our first set of experiments we tested constructs that included only the head and neck domains, including charged regions. We then prolonged them gradually by adding multiples of heptad repeats until we reached the end of coiled-coil region III (FIP motive; Figures 3 and 7). It soon became evident that the critical regions for Xklp3A/B heterodimer formation cannot be found at the N-terminal regions of the stalk, but locate towards the C-terminus, at the very end of the coiled coil. N-terminal truncations, on the other hand, made clear that heterodimer formation occurs with constructs lacking the entire charged region, coiled-coil I and even a substantial portion of coiled-coil region II. This clearly excludes an involvement of the neck and charged region in the process of heterodimer initiation (Figures 3 and 7).

Our results indicate that successful heterodimer formation requires about four consecutive heptad repeats in coiled-coil region II interacting cooperatively with the entire coiled-coil region III (six heptads; Figures 4–6; see also Figure 3). However, this result certainly depends on actual concentrations. Our experiments are performed in the near-physiological environment of reticulocyte lysates after overexpression. It may well be that at actual concentrations such as are found *in vivo* the required stretch of coiled-coil segment II has to be even longer for a successful dimer formation. In any case, neither of the two C-terminal coiled-coil regions by themselves seems to have a high enough coiled-coil propensity to induce heterodimer formation, but need to interact in a cooperative manner. Here we found that if the critical region is truncated by only one heptad repeat (Figure 4B) from either end, the coiled-coil propensity drops below a critical level for dimer formation under physiological conditions (see Figure 4B and C).

Functional implications of the kinesin-II heterodimer formation properties

Conventional kinesin and kinesin-II both form dimeric complexes mediated by a coiled-coil interaction. The mechanisms of dimer formation, however, are strikingly different from each other. Conventional kinesin forms a stable dimer in the absence of most of its C-terminal stalk regions. The first 35 amino acids of the neck helices have been demonstrated to mediate dimer formation (Morii *et al*., 1997; Marx *et al*., 1998; Thormählen *et al*., 1998). Thormählen *et al*. (1998) proposed a potential coiled-coil trigger site located at the C-terminal end of the neck helix. Our results presented here now suggest that dimer formation of kinesin-II is very different from conventional kinesin and is distinguished by the following aspects. (i) Neither Xklp3A nor Xklp3B forms homodimers (Figure 6). (ii) The neck region of the Xklp3A/B complex is not directly involved in (hetero)dimer formation (Figures 5 and 6). Its own coiled-coil propensity is very low. (iii) The regions that are essential for kinesin-II dimerization are located towards the C-terminal end of the stalk (Figures 4–6). (iv) Dimerization is not mediated by a trigger site, but appears to be initiated by a cooperative interaction between the two C-terminally located coiled-coil domains. And finally, (v) coiled-coil region I and the charged stretches do not appear to play any role in the initiation or stabilization of heterodimer formation.

Our work does not provide an answer to potential functions of the oppositely charged stretches located at the beginning of the kinesin-II stalk. These stretches have been proposed previously to play a key role in heterodimer formation for motor domain complex formation in kinesin-II (Rashid *et al*., 1995), and its characteristic structure may suggest exactly that. However, we found that this is clearly not the case for Xklp3A/B heterodimer formation, a finding that we believe might well apply to all members of the kinesin-II family. The charged regions may be omitted on both chains. They are not essential for heterodimer formation, nor do constructs that lack the charged stretches tend to form homodimers instead (see Figure 6). One could speculate about other functions of the charged regions that relate to a mechanism suggested recently by Thorn *et al*. (2000). Their work suggests a functional interaction between charged elements of the conventional kinesin stalk and the C-terminal ends of α- and β-tubulin, thereby promoting a one-dimensional diffusion of kinesins along microtubules even in the absence of ATP hydrolysis.

Interestingly, the critical regions for heterodimer formation (C-terminal half of coiled-coil II and the entire coiled-coil region III) exhibit a much higher degree of conservation among the related members of the kinesin-II family (Xklp3A, KIF3A, KRP85) than coiled-coil region I, neck and charged stretches (Figure 1B). The same is true among their partners (Xklp3B, KIF3B and KRP95). This suggests that neck and charged region show a more specific adjustment to the individual functions of each member while the critical regions for dimerization remain preserved for a more universal and flexible role in heterodimer formation. In addition, the Xklp3A/B complex formation is controlled by a rather weak coiled-coil interaction, which, among kinesins, seems to constitute a unique and typical property of kinesin-II. Unlike for a dimerization mediated by a trigger site or any short but strong stretch of coiled coil, the mechanism proposed here may leave a higher degree of flexibility with regard to heterodimeric partners, and at the same time prevent homodimer formation. The detailed structural mechanisms of dimer formation, however, remain unclear. It will be very important to monitor the structural changes involved in monomer–dimer transition (e.g. by CD spectroscopy or kinetic analyses), and to clarify its regulation in a cell. It is

also still unclear how the trimeric complex (including cargo domain) forms. These investigations will be possible once both chains can be individually expressed and purified *in vitro* and analysed in more detail.

Materials and methods

Cloning of Xklp3A

Conserved sequences from the motor and tail domains of MmKIF3A were used for a BLAST search in a human expressed sequence tag (EST) database. The chosen ESTs, corresponding to the motor (DDBJ/EMBL/GenBank accession No. AI267716) and tail regions (H97461) of the putative human KIF3A were used to screen a mature *Xenopus* oocyte cDNA library in λ-ZAP (for details see Wittmann *et al*., 2000). Several independent clones were isolated, excised and sequenced. The clones contained overlapping sequences lacking the 3′ end of Xklp3A open reading frame (ORF). This last missing portion was obtained using a SMART RACE protocol (Clontech, Palo Alto, CA). The complete Xklp3A gene was obtained by PCR on cDNA prepared from the total RNA of XL177 cells, and cloned directly into the pCR2.1 vector using the TA cloning kit (Invitrogen, Groningen, The Netherlands). The clone was sequenced on both strands and confirmed to have one ORF. The Xklp3A cDNA sequence can be found in the DDBJ/EMBL/GenBank database under accession No. AJ311602. The Xklp3A predicted protein sequence was aligned to SpKRP85 (L16993) and MmKIF3A (D12645) using ClustalX (Figure 1B; Jeanmougin *et al*., 1998).

Engineering of stalk fragments at various lengths

Untagged Xklp3A constructs were obtained by PCR on Xklp3A full-length clone and cloned directly into the pCR2.1 vector, using the TA cloning kit (Invitrogen). All constructs were tested by digestion to check for correct orientation into the vector and sequenced. GST fusion constructs were generated by PCR, introducing *Bam*HI and *Xho*I sites at the 5′ and 3′ ends, respectively, cloned into the pGAT vector (Peränen *et al*., 1996) and sequenced for verification of completeness and correct insertion.

Immunoprecipitation experiments

To test the Xklp3A–Xklp3B interaction, Xklp3A and Xklp3B were transcribed and translated either separately or simultaneously in a coupled rabbit reticulocyte lysate system (Promega, Madison, WI) for 90 min at 30°C in the presence of [^{35}S]methionine. Protein A support beads (Bio-Rad, Hercules, CA) were washed and saturated with phosphate-buffered saline (PBS), 2% bovine serum albumin (BSA), 0.1% Triton X-100, then coated with either an α-KRP85 antibody (K2.4, Hiss Diagnostics, Freiburg, Germany) or an α-Xklp3B antibody (Le Bot *et al*., 1998) by rolling for 1 h at 4°C. After coupled transcription–translation, crude lysates were incubated with the coated beads for 1 h at 4°C. Beads were washed with PBS, 0.1% Triton X-100. The immunoprecipitates were then eluted by boiling the samples in SDS–PAGE sample buffer. Samples were separated by SDS–PAGE; gels were dried and subsequently exposed for 12 h at –70°C (BioMax MR-1 film, Kodak, St Louis, MO).

Similarly, Xklp3B was co-expressed with each of the untagged Xklp3A constructs in the reticulocyte lysate system. Reticulocyte lysates were then incubated with beads coated with either an α-KRP85 antibody or an α-Xklp3B antibody for 1 h at 4°C. Immunoprecipitates were analysed by SDS–PAGE. Gels were recorded by autoradiography as described above. When GST fusion constructs were used, immunoprecipitation tests were performed using an α-GST antibody (kindly provided by T.Wittmann, Scripps Institute, La Jolla, CA) (Wittmann *et al*., 1998), anything else following the procedure described.

The same procedure was followed in reverse order to co-express Xklp3A with GST–Xklp3B constructs for verification of the previous results.

Acknowledgements

We are very grateful to Ann Westerholm-Parvinen (Cell Biology and Cell Biophysics Programme, EMBL, Heidelberg, Germany) for continuous support, advice and suggestions and to Professor Ueli Aebi (Biocenter, University of Basel, Switzerland) and Eckhard Mandelkow (MPG, DESY-Hamburg, Germany) for helpful discussions.

References

Arndt,K.M., Pelletier,J.N., Muller,K.M., Alber,T., Michnick,S.W. and Pluckthun,A. (2000) A heterodimeric coiled-coil peptide pair selected *in vivo* from a designed library-versus-library ensemble. *J. Mol. Biol.*, **295**, 627–639.

Brady,S.T. (1985) A novel brain ATPase with properties expected for the fast axonal transport motor. *Nature*, **317**, 73–75.

Brown,J.H., Cohen,C. and Parry,D.A. (1996) Heptad breaks in α-helical coiled coils: stutters and stammers. *Proteins*, **26**, 134–145.

Brown,J.M., Marsala,C., Kosoy,R. and Gaertig,J. (1999) Kinesin-II is preferentially targeted to assembling cilia and is required for ciliogenesis and normal cytokinesis in *Tetrahymena*. *Mol. Biol. Cell*, **10**, 3081–3096.

Burkhard,P., Kammerer,R.A., Steinmetz,M.O., Bourenkov,G.P. and Aebi,U. (2000a) The coiled-coil trigger site of the rod domain of cortexillin I unveils a distinct network of interhelical and intrahelical salt bridges. *Struct. Fold. Des.*, **8**, 223–230.

Burkhard,P., Meier,M. and Lustig,A. (2000b) Design of a minimal protein oligomerization domain by a structural approach. *Protein Sci.*, **9**, 2294–2301.

Cole,D.G., Chinn,S.W., Wedaman,K.P., Hall,K., Vuong,T. and Scholey,J.M. (1993) Novel heterotrimeric kinesin-related protein purified from sea urchin eggs. *Nature*, **366**, 268–270.

Cole,D.G., Diener,D.R., Himelblau,A.L., Beech,P.L., Fuster,J.C. and Rosenbaum,J.L. (1998) *Chlamydomonas* kinesin-II-dependent intraflagellar transport (IFT): IFT particles contain proteins required for ciliary assembly in *Caenorhabditis elegans* sensory neurons. *J. Cell Biol.*, **141**, 993–1008.

Hirokawa,N. (1998) Kinesin and dynein superfamily proteins and the mechanism of organelle transport. *Science*, **279**, 519–526.

Jeanmougin,F., Thompson,J.D., Gouy,M., Higgins,D.G. and Gibson,T.J. (1998) Multiple sequence alignment with Clustal X. *Trends Biochem. Sci.*, **23**, 403–405.

Kammerer,R.A., Schulthess,T., Landwehr,R., Lustig,A., Engel,J., Aebi,U. and Steinmetz,M.O. (1998) An autonomous folding unit mediates the assembly of two-stranded coiled coils. *Proc. Natl Acad. Sci. USA*, **95**, 13419–13424.

Kondo,S., Sato-Yoshitake,R., Noda,Y., Aizawa,H., Nakata,T., Matsuura,Y. and Hirokawa,N. (1994) KIF3A is a new microtubule-based anterograde motor in the nerve axon. *J. Cell Biol.*, **125**, 1095–1107.

Kozielski,F., Sack,S., Marx,A., Thormählen,M., Schonbrunn,E., Biou,V., Thompson,A., Mandelkow,E.M. and Mandelkow,E. (1997) The crystal structure of dimeric kinesin and implications for microtubule-dependent motility. *Cell*, **91**, 985–994.

Le Bot,N., Antony,C., White,J., Karsenti,E. and Vernos,I. (1998) Role of Xklp3, a subunit of the *Xenopus* kinesin II heterotrimeric complex, in membrane transport between the endoplasmic reticulum and the Golgi apparatus. *J. Cell Biol.*, **143**, 1559–1573.

Marszalek,J.R. and Goldstein,L.S. (2000) Understanding the functions of kinesin-II. *Biochim. Biophys. Acta*, **1496**, 142–150.

Marx,A., Thormählen,M., Muller,J., Sack,S., Mandelkow,E.M. and Mandelkow,E. (1998) Conformations of kinesin: solution vs. crystal structures and interactions with microtubules. *Eur. Biophys. J.*, **27**, 455–465.

Morii,H., Takenawa,T., Arisaka,F. and Shimizu,T. (1997) Identification of kinesin neck region as a stable α-helical coiled coil and its thermodynamic characterization. *Biochemistry*, **36**, 1933–1942.

Morris,R.L. and Scholey,J.M. (1997) Heterotrimeric kinesin-II is required for the assembly of motile 9+2 ciliary axonemes on sea urchin embryos. *J. Cell Biol.*, **138**, 1009–1022.

Muresan,V., Abramson,T., Lyass,A., Winter,D., Porro,E., Hong,F., Chamberlin,N.L. and Schnapp,B.J. (1998) KIF3C and KIF3A form a novel neuronal heteromeric kinesin that associates with membrane vesicles. *Mol. Biol. Cell*, **9**, 637–652.

Nonaka,S., Tanaka,Y., Okada,Y., Takeda,S., Harada,A., Kanai,Y., Kido,M. and Hirokawa,N. (1998) Randomization of left–right asymmetry due to loss of nodal cilia generating leftward flow of extraembryonic fluid in mice lacking KIF3B motor protein. *Cell*, **95**, 829–837.

Peränen,J., Rikkonen,M., Hyvönen,M. and Kääriäinen,L. (1996) T7 vectors with modified T7lac promoter for expression of proteins in *Escherichia coli*. *Anal. Biochem.*, **236**, 371–373.

Rashid,D.J., Wedaman,K.P. and Scholey,J.M. (1995) Heterodimerization of the two motor subunits of the heterotrimeric kinesin, KRP85/95. *J. Mol. Biol.*, **252**, 157–162.

Ray,K., Perez,S.E., Yang,Z., Xu,J., Ritchings,B.W., Steller,H. and Goldstein,L.S. (1999) Kinesin-II is required for axonal transport of choline acetyltransferase in *Drosophila*. *J. Cell Biol.*, **147**, 507–518.

Rosenbaum,J.L., Cole,D.G. and Diener,D.R. (1999) Intraflagellar transport: the eyes have it. *J. Cell Biol.*, **144**, 385–388.

Sack,S., Kull,F.J. and Mandelkow,E. (1999) Motor proteins of the kinesin family. Structures, variations and nucleotide binding sites. *Eur. J. Biochem.*, **262**, 1–11.

Scholey,J.M. (1996) Kinesin-II, a membrane traffic motor in axons, axonemes and spindles. *J. Cell Biol.*, **133**, 1–4.

Signor,D., Wedaman,K.P., Rose,L.S. and Scholey,J.M. (1999a) Two heteromeric kinesin complexes in chemosensory neurons and sensory cilia of *Caenorhabditis elegans*. *Mol. Biol. Cell*, **10**, 345–360.

Signor,D., Wedaman,K.P., Orozco,J.T., Dwyer,N.D., Bargmann,C.I., Rose,L.S. and Scholey,J.M. (1999b) Role of a class DHC1b dynein in retrograde transport of IFT motors and IFT raft particles along cilia, but not dendrites, in chemosensory neurons of living *Caenorhabditis elegans*. *J. Cell Biol.*, **147**, 519–530.

Steinmetz,M.O., Stock,A., Schulthess,T., Landwehr,R., Lustig,A., Faix,J., Gerisch,G., Aebi,U. and Kammerer,R.A. (1998) A distinct 14 residue site triggers coiled-coil formation in cortexillin I. *EMBO J.*, **17**, 1883–1891.

Strelkov,S.V., Herrmann,H., Geisler,N., Lustig,A., Zimbelmann,R., Burkhard,P. and Aebi,U. (2001) 'Divide-and-conquer' crystallographic approach towards an atomic structure of intermediate filaments. *J. Mol. Biol.*, **306**, 773–781.

Tabish,M., Siddiqui,Z.K., Nishikawa,K. and Siddiqui,S.S. (1995) Exclusive expression of *C. elegans osm-3* kinesin gene in chemosensory neurons open to the external environment. *J. Mol. Biol.*, **247**, 377–389.

Thormählen,M., Marx,A., Sack,S. and Mandelkow,E. (1998) The coiled-coil helix in the neck of kinesin. *J. Struct. Biol.*, **122**, 30–41.

Thorn,K.S., Ubersax,J.A. and Vale,R.D. (2000) Engineering the processive run length of the kinesin motor. *J. Cell Biol.*, **151**, 1093–1100.

Tripet,B., Wagschal,K., Lavigne,P., Mant,C.T. and Hodges,R.S. (2000). Effects of side-chain characteristics on stability and oligomerization state of a de novo-designed model coiled-coil: 20 amino acid substitutions in position 'd'. *J. Mol. Biol.*, **300**, 377–402

Tuma,M.C., Zill,A., Le Bot,N., Vernos,I. and Gelfand,V. (1998) Heterotrimeric kinesin II is the microtubule motor protein responsible for pigment dispersion in *Xenopus* melanophores. *J. Cell Biol.*, **143**, 1547–1558.

Vale,R.D., Reese,T.S. and Sheetz,M.P. (1985) Identification of a novel force-generating protein, kinesin, involved in microtubule-based motility. *Cell*, **42**, 39–50.

Vernos,I., Heasman,J. and Wylie,C. (1993) Multiple kinesin-like transcripts in *Xenopus* oocytes. *Dev. Biol.*, **157**, 232–239.

Wedaman,K.P., Meyer,D.W., Rashid,D.J., Cole,D.G. and Scholey,J.M. (1996) Sequence and submolecular localization of the 115-kD accessory subunit of the heterotrimeric kinesin-II (KRP85/95) complex. *J. Cell Biol.*, **132**, 371–380.

Wittmann,T., Boleti,H., Antony,C., Karsenti,E. and Vernos,I. (1998) Localization of the kinesin-like protein Xklp2 to spindle poles requires a leucine zipper, a microtubule-associated protein and dynein. *J. Cell Biol.*, **143**, 673–685.

Wittmann,T., Wilm,M., Karsenti,E. and Vernos,I. (2000) TPX2, A novel *Xenopus* MAP involved in spindle pole organization. *J. Cell Biol.*, **149**, 1405–1418.

Wolf,E., Kim,P.S. and Berger,B. (1997) MultiCoil: a program for predicting two- and three-stranded coiled coils. *Protein Sci.*, **6**, 1179–1189.

Yamazaki,H., Nakata,T., Okada,Y. and Hirokawa,N. (1995) KIF3A/B: a heterodimeric kinesin superfamily protein that works as a microtubule plus end-directed motor for membrane organelle transport. *J. Cell Biol.*, **130**, 1387–1399.

Yang,Z. and Goldstein,L.S. (1998) Characterization of the KIF3C neural kinesin-like motor from mouse. *Mol. Biol. Cell*, **9**, 249–261.

Received March 28, 2001; revised May 2, 2001;
accepted May 10, 2001